SUNY COLLEGE OF NANOSCALE SCIENCE AND ENGINEERING

Potential *in situ* characterization of physical vapor deposition of CIGS film growth at ISR and other relevant NSLS-II beamlines

Richard J. Matyi[1] and Kenneth Evans-Lutterodt[2]

[1]SUNY College of Nanoscale Science and Engineering
Albany, NY 12203

[2] Brookhaven National Laboratory
Upton, NY 11973

Agenda

- A CIGS primer
- Physical vapor deposition 101
- CIGS PVD
- Rietveld analysis of structure development in CIGS
- The need for synchrotron *in situ* analyses
- Expected outcomes from an *in situ* PVD capability on the ISR beamline

A CIGS primer

- CIGS (Copper Indium Gallium Selenium) photovoltaic materials are currently one of the leaders in the solar cell industry due to their relatively high efficiency
- CIGS has a complex structure, due to the multiple deposition steps (a "three stage" physical vapor deposition process shown on the right is commonly used)
- The Ga and In occupy the same site in the crystal lattice, giving another unpredictable variable

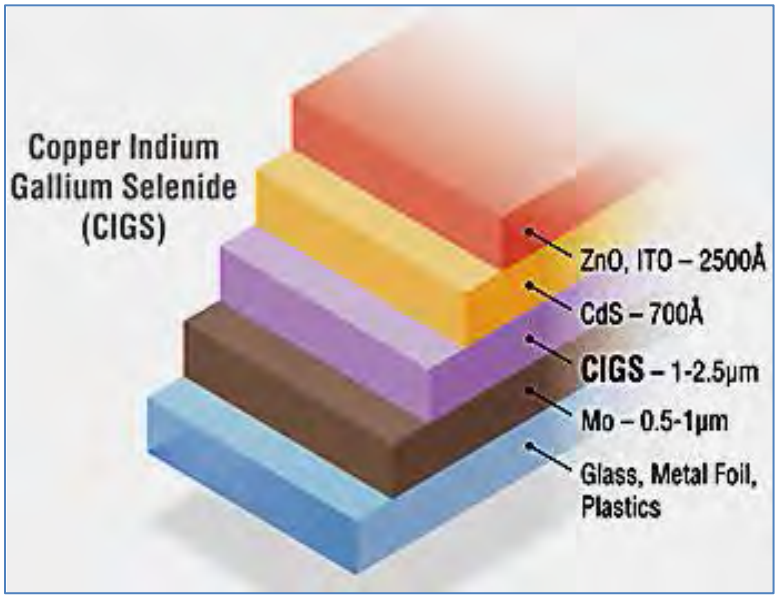

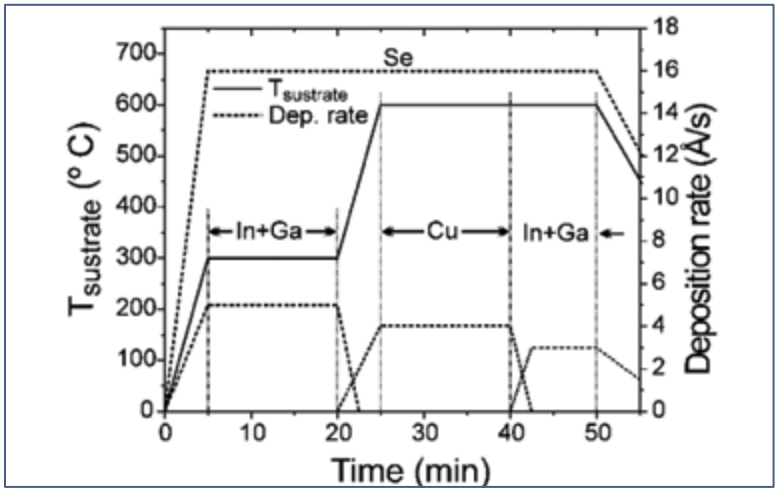

A CIGS primer (con't)

- The gallium and indium occupy the same site in the crystal lattice, giving another unpredictable variable
- A back electrical contact of molybdenum is typically employed
- Preferred orientation may play a crucial role in determining the efficiency of the material – this is a difficult variable to isolate
- CIGS growth is typically achieved via physical vapor deposition: a process that is simple to perform but difficult to understand
  - Nanostructure versus microstructure: will compete to control properties

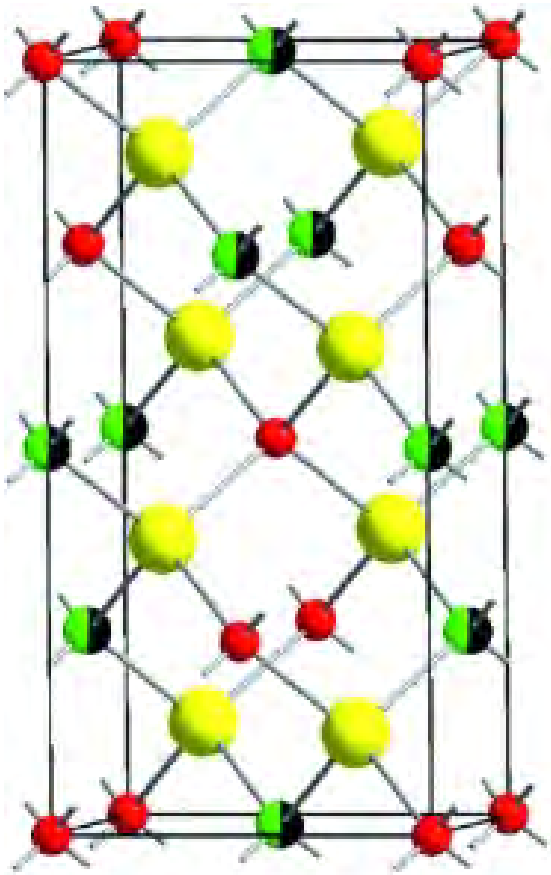

$Cu(In,Ga)Se_2$

The complete CIGS PV cell environment

CIGS Unit Film Fabrication & Characterization @ CNSE/PVMC

Indepth analysis required

Grids: Diffusion of Al, Ag & Ni

Window layer: Sputtering damage to the junction

Buffer Layer: Pin holes, Diffusion into window and absorber layer

(Element specific)
Surface, Bulk Composition
Depth profile, Defects,
Elements present in Grain boundaries, Na concentration,

Contaminants from substrate (Glass/Stainless steel), Film stress CIGS/Mo interface , adhesion

Qualitative analysis of surface defects (Micro and Macro level)
Surface roughness & composition

Interface properties

Goal : Correlate properties with performance metrics

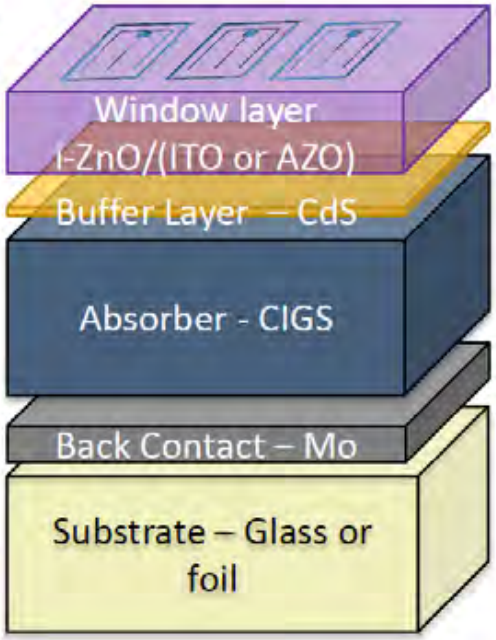

Fabrication Method

Grids: Evaporation
Ni (150-500A) Ag (5000-6000A)
Al(2-3µ); screen print; applied

Window layer: Sputter
Resistive: i-ZnO 50-100nm
Conductive:ITOorAZO- 0.3-1.2µ

Buffer Layer: Chemical bath deposition (CBD)/Sputter: CdS, Zn(O,S); 20-50nm;

CIGS: Cu, In, Ga are Co-evaporated in Se overpressure CIGS- ~1-2µ

Molybdenum-Sputter; ~0.3-1µ
Barrier layers: Cr

Glass: 2 to 3.2mm
Stainless foil: 25 to 125um

Deposition methods & Thickness

Physical vapor deposition 101

- The development of microstructure in a thin film deposited from the vapor phase is a complex process that initially involves:
  - transport of atoms from the vapor phase to the vicinity of a surface
  - condensation of atoms onto the surface
  - surface diffusion of the adsorbed atoms
  - incorporation of source atoms into a growing film via (a) nucleation of isolated islands, (b) island growth, and (c) the impingement and coalescence of islands
- As the film grows thicker, the morphology of the film may evolve by
  - formation of polycrystalline islands and channels
  - the development of a continuous film
  - local epitaxy on grains and columns
  - competitive column growth and grain coarsening
- All of this will proceed with the local chemistry of the site occupancy in the nanoscale unit cell

Physical vapor deposition 101

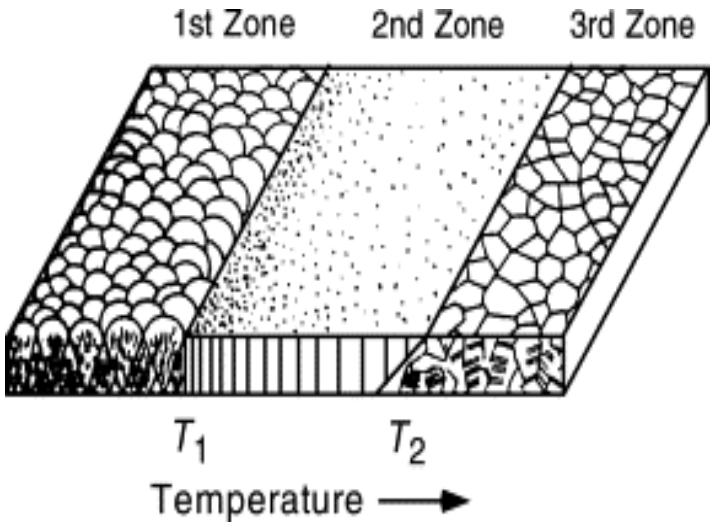

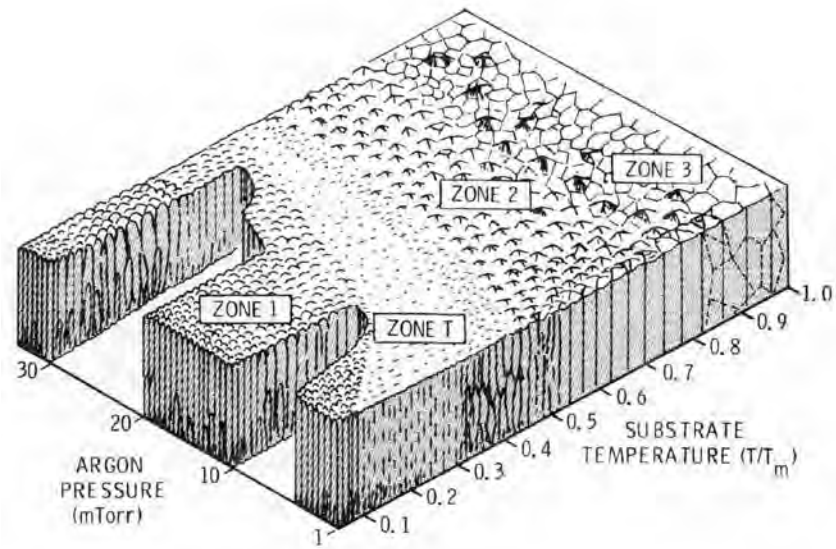

- The "structure zone model" gives a representation of the cumulative effects of the kinetic factors that control PVD film growth
- Illustrates the morphology that develops as a function of the homologous temperature (ratio of the absolute substrate temperature to the absolute melting temperature: T/T_m)

Grain growth and texture development

- In polycrystalline structures a driving force for the development of polycrystalline grain structure is the minimization of surface energies of the free surface (γ_f), the interface (γ_i) and the grain boundaries (γ_{gb})
- Surface and interface energy minimization can result in the growth of grains with preferred orientations or textures
- Systems with complex chemistry (e.g. quaternaries) would be expected to show complex behavior due to interface enrichment
- Still more complications due to strains (homogeneous vs. inhomogeneous)

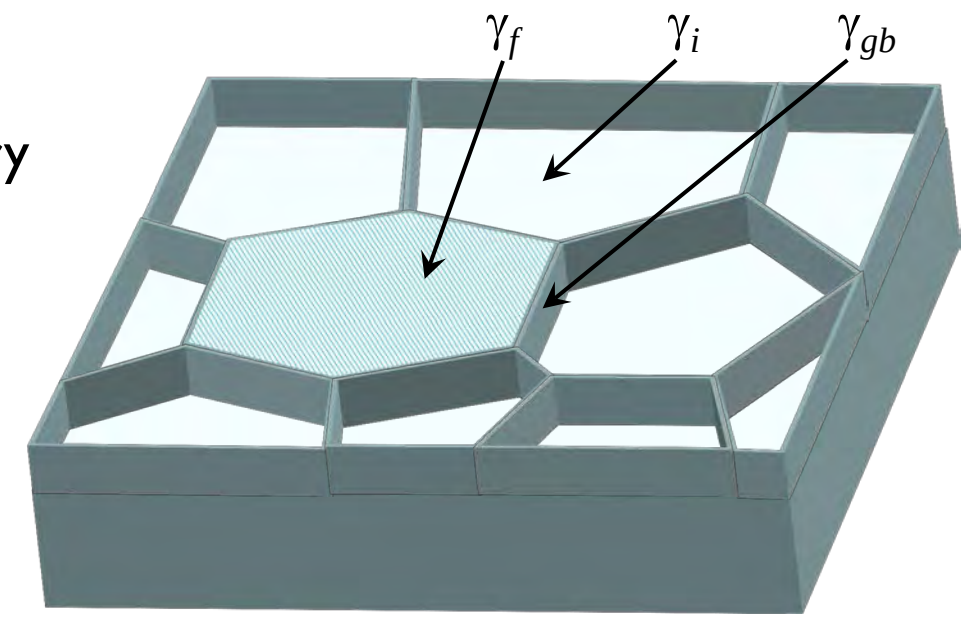

Scientific foundations of CIGS deposition

- Background
  - The equilibrium properties of CIGS materials (composition; band structure) on PV properties are well understood
  - In contrast, the evolution of materials structure and its resultant impact on performance depends on the kinetics of the deposition process is poorly characterized
- Critical kinetic factors in multicomponent (quaternary) deposition can be identified
  - Competing surface diffusion processes will control sublattice chemical incorporation and alter electronic structure (sensitive to sputtering versus vacuum evaporation)
  - Growth rate competes with interfacial energy (dependent on solute segregation) to determine crystallographic texture
  - Growth-induced defect incorporation may (or may not) impact nominal bulk characteristics of CIGS materials

CIGS deposition: research needs

- The fundamental kinetic processes that control structure and properties in simple single-component PVD systems are well understood (example: molybdenum)
- In contrast: the kinetic factors in quaternary CIGS growth are poorly understood at a fundamental level
  - competing surface diffusion versus incorporation and growth
  - composition-dependent surface energy control of grain growth and the development of texture
  - defect generation dependence on growth kinetics
- Understanding the impact of kinetic factors on the growth process leads to a fundamental understanding of the relation between structure, properties and performance in thin film systems
  - Example: the development of manufacturing processes for advanced hard disc drives followed a detailed understanding of the PVD deposition processes of single-component systems

SUNY College of Nanoscale Science and Engineering

XRF mapping of CIGS/Mo

%Cu

21.84	22.27	22.17	22.24	22.29	22.4	22.5	22.77
21.74	21.84	22.2	21.94	22.47	22.27	22.46	22.46
21.84	22.33	22.5	22.17	22.72	22.6	22.46	22.58
22.1	22.25	22.24	22.32	22.18	22.34	22.42	22.23
21.77	22.03	22.03	22.36	22.2	22.29	21.95	22.51
21.78	22.14	21.84	22.32	22.27	22.4	22.06	22.12
21.56	21.95	21.65	22.23	22.21	22.02	22.3	22.41
21.5	22.15	21.54	22.06	21.96	22.23	22.27	22.28
21.82	22	21.73	22	22.04	21.81	22.18	21.94
21.51	22.05	21.81	21.81	21.78	22.11	22.2	21.9
21.46	21.53	21.62	21.83	21.86	21.83	22.06	21.93
21.3	21.47	21.42	21.74	21.68	21.79	22.41	21.82

%Ga

8.646	8.686	8.53	8.434	8.282	8.472	8.496	8.375
8.531	8.407	8.41	8.226	8.321	8.255	8.154	8.272
8.445	8.304	8.391	8.185	8.297	8.202	8.128	8.274
8.313	8.238	8.023	8.153	8.018	8.035	8.032	8.032
8.198	8.136	8.01	7.983	8.015	7.921	7.917	7.819
8.146	8.025	7.886	7.94	7.842	7.786	7.685	7.887
7.965	7.834	7.848	7.785	7.748	7.577	7.559	7.694
7.925	7.686	7.67	7.67	7.586	7.526	7.533	7.562
7.778	7.838	7.579	7.572	7.481	7.402	7.364	7.38
7.637	7.662	7.596	7.414	7.368	7.398	7.381	7.415
7.601	7.406	7.3	7.461	7.24	7.221	7.198	7.325
7.416	7.391	7.213	7.265	7.231	7.087	7.242	7.158

Cu/(In+Ga)

0.828	0.872	0.844	0.834	0.847	0.872	0.869	0.885
0.827	0.813	0.836	0.813	0.873	0.831	0.852	0.861
0.829	0.867	0.871	0.829	0.903	0.876	0.857	0.876
0.838	0.846	0.85	0.836	0.827	0.857	0.852	0.834
0.811	0.821	0.819	0.849	0.854	0.837	0.831	0.852
0.807	0.848	0.805	0.842	0.822	0.856	0.815	0.839
0.792	0.814	0.795	0.851	0.831	0.791	0.828	0.845
0.79	0.829	0.781	0.831	0.795	0.818	0.836	0.846
0.803	0.841	0.79	0.826	0.804	0.789	0.82	0.803
0.779	0.823	0.808	0.798	0.791	0.811	0.828	0.808
0.788	0.777	0.784	0.823	0.81	0.802	0.812	0.811
0.772	0.775	0.758	0.793	0.787	0.785	0.849	0.807

Se/(Cu+In+Ga)

1.075	1.092	1.065	1.045	1.057	1.08	1.067	1.062
1.083	1.053	1.051	1.043	1.074	1.038	1.049	1.059
1.075	1.079	1.07	1.044	1.088	1.067	1.055	1.069
1.064	1.059	1.067	1.04	1.04	1.065	1.053	1.045
1.056	1.046	1.044	1.053	1.074	1.045	1.068	1.043
1.051	1.073	1.042	1.048	1.027	1.058	1.036	1.062
1.049	1.044	1.045	1.068	1.044	1.005	1.032	1.044
1.053	1.046	1.036	1.057	1.016	1.025	1.044	1.056
1.041	1.076	1.031	1.056	1.023	1.022	1.031	1.03
1.036	1.047	1.049	1.035	1.028	1.025	1.041	1.041
1.054	1.03	1.033	1.069	1.048	1.039	1.031	1.043
1.046	1.033	1.013	1.035	1.031	1.018	1.05	1.046

%In

17.72	16.85	17.74	18.23	18.04	17.2	17.39	17.34
17.74	18.47	18.15	18.77	17.42	18.54	18.19	17.83
17.91	17.46	17.43	18.56	16.86	17.58	18.08	17.49
18.05	18.06	18.13	18.55	18.81	18.05	18.27	18.63
18.66	18.7	18.88	18.36	17.99	18.7	18.5	18.61
18.83	18.07	19.24	18.56	19.23	18.4	19.38	18.49
19.27	19.13	19.4	18.34	18.97	20.28	19.36	18.81
19.29	19.04	19.92	18.89	20.04	19.64	19.13	18.79
19.4	18.33	19.93	19.06	19.92	20.24	19.69	19.94
19.98	19.13	19.4	19.93	20.17	19.86	19.42	19.68
19.63	20.31	20.26	19.05	19.73	19.99	19.98	19.71
20.17	20.32	21.05	20.14	20.32	20.69	19.14	19.88

%Se

51.8	[illegible]	51.57	51.09	51.39	51.93	51.61	51.51
51.99	51.28	51.06	51.79	50.93	51.2	51.43	51.66
51.8	51.91	51.68	51.09	52.12	51.62	51.33	51.33
51.54	51.44	51.61	50.98	50.99	51.57	51.28	51.11
51.37	51.13	51.08	51.3	51.79	51.09	51.64	51.05
51.24	51.76	51.04	51.18	50.66	51.41	50.87	51.49
51.2	51.08	51.1	51.64	51.07	50.12	50.79	51.08
51.29	51.13	50.88	51.38	50.41	50.61	51.07	51.37
51	51.83	50.76	51.37	50.56	50.54	50.77	50.74
50.87	51.16	51.19	50.85	50.68	50.63	51	51.01
51.31	50.75	50.82	51.66	51.17	50.97	50.76	51.04
51.11	50.82	50.32	50.85	50.77	50.44	51.21	51.14

Ga/(In+Ga)

0.328	0.34	0.325	0.316	0.315	0.33	0.328	0.326
0.325	0.313	0.317	0.305	0.323	0.308	0.31	0.317
0.32	0.322	0.325	0.306	0.33	0.318	0.31	0.321
0.315	0.313	0.307	0.305	0.299	0.308	0.305	0.301
0.305	0.303	0.298	0.303	0.308	0.298	0.3	0.296
0.302	0.307	0.291	0.3	0.29	0.297	0.284	0.299
0.292	0.291	0.288	0.298	0.29	0.272	0.281	0.29
0.291	0.288	0.278	0.289	0.275	0.277	0.283	0.287
0.286	0.299	0.275	0.284	0.273	0.268	0.272	0.27
0.277	0.286	0.281	0.271	0.268	0.271	0.275	0.274
0.279	0.267	0.265	0.281	0.268	0.265	0.265	0.271
0.269	0.267	0.255	0.265	0.262	0.255	0.275	0.265

Cu thickness

1.799	1.833	1.886	1.928	1.937	1.908	1.903	1.866
1.852	1.922	1.954	1.987	1.959	1.988	1.974	1.939
1.896	1.932	1.953	2.017	1.976	2.008	2.017	1.958
1.913	1.974	2.009	2.056	2.072	1.99	2.014	2.026
1.97	2.011	2.051	2.062	2.075	2.093	2.064	2.032
1.97	2.012	2.093	2.106	2.135	2.12	2.11	2.058
2.025	2.068	2.11	2.108	2.133	2.196	2.158	2.086
2.03	2.086	2.139	2.136	2.194	2.181	2.15	2.092
2.039	2.071	2.151	2.156	2.201	2.216	2.189	2.143
2.066	2.095	2.153	2.2	2.211	2.205	2.175	2.145
2.039	2.146	2.171	2.15	2.193	2.197	2.188	2.143
2.051	2.122	2.188	2.18	2.195	2.208	2.16	2.13

- XRF measurements made at PVMC on the same sample show spatial variations that appear to correlate with XRD results

Rietveld refinement

- We have implemented Rietveld whole pattern refinement methods for quantitative X-ray diffraction structural analyses of CIGS materials
- Rietveld refinement programs use least squares fits of an XRD pattern to refine structural, chemical and instrumental parameters for a single phase using:

$$I_i^{\text{calc}} = \sum_{k=1}^{M\ \text{peaks}} L_k \left|F_k\right|^2 S(2\theta_i - 2\theta_k) P_k A + bkg_i$$

number of peaks

angular corrections

structure factor

peak shape function

preferred orientation

absorption correction

background

- The structure factor F_{hkl} contains all crystal information for a phase (space group, atomic positions, lattice parameter, site occupancy, thermal vibrations); absorption and preferred orientation included separately
- Current work performed on a laboratory diffractometer

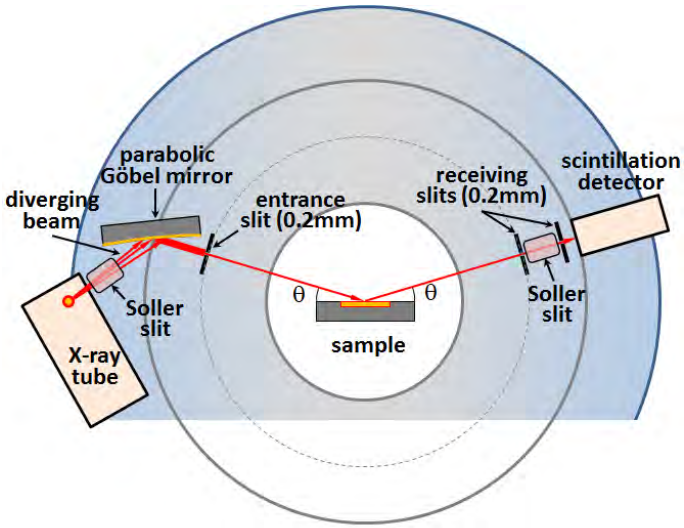

An example: structure evolution in CIGS

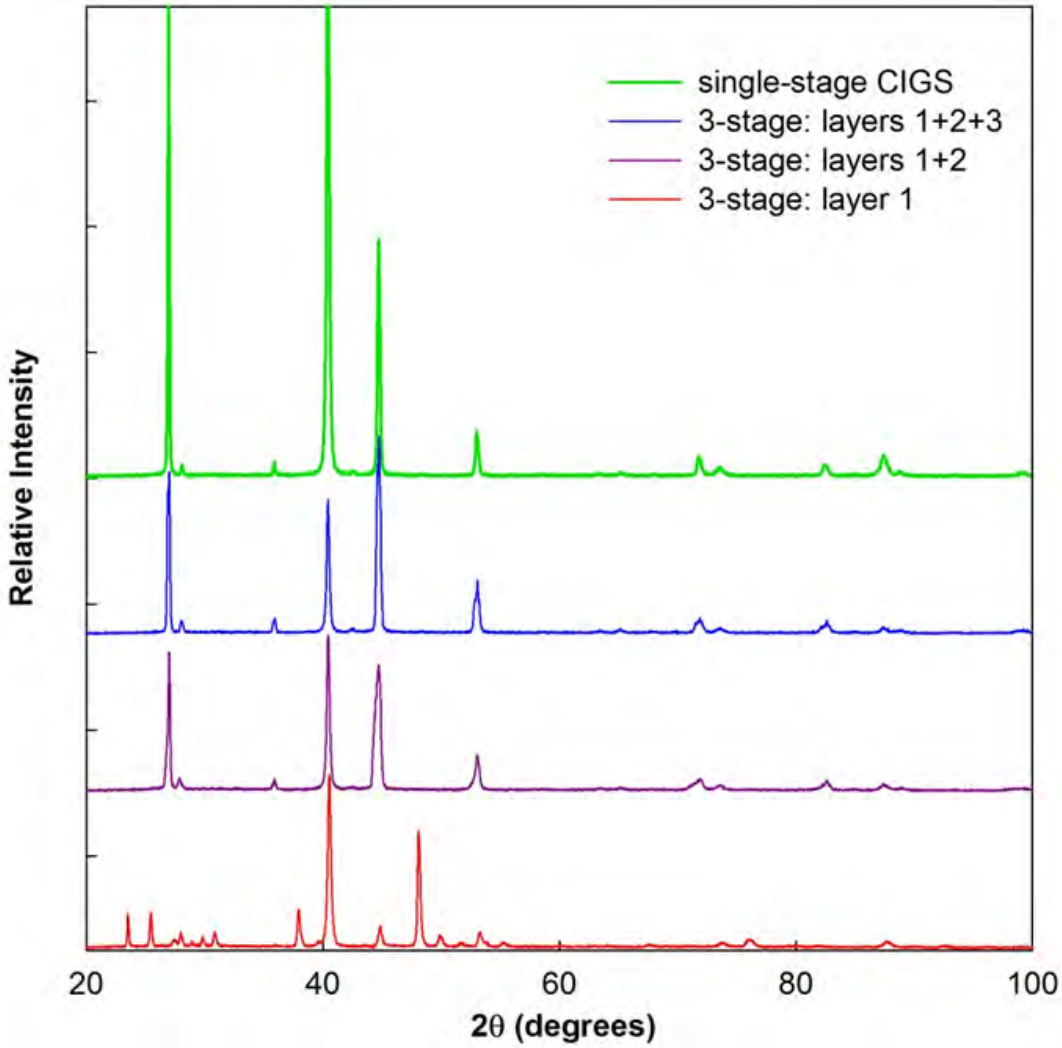

- Experimental XRD scans were recorded from a variety of CIGS samples:
  - single-stage, four-component deposition
  - three-stage CIGS samples with growth interruptions at each stage (1st layer, 1st + 2nd layer, 1st + 2nd + 3rd layers)
- All deposition performed on Mo back contact layers
- Thick layers on SLG: good candidates for analysis via Rietveld refinement

Detail of CIGS (220) and Mo (110) reflections

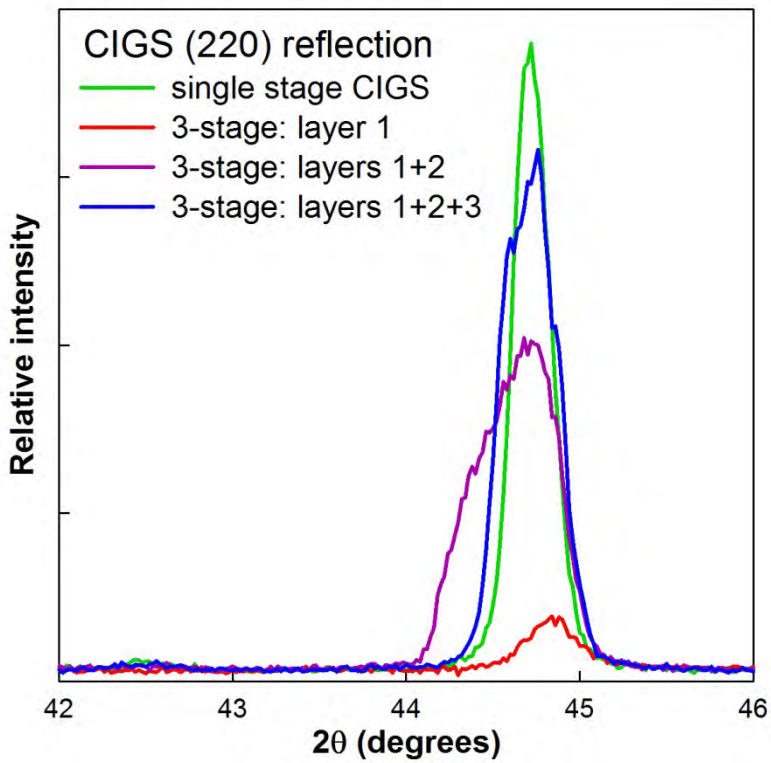

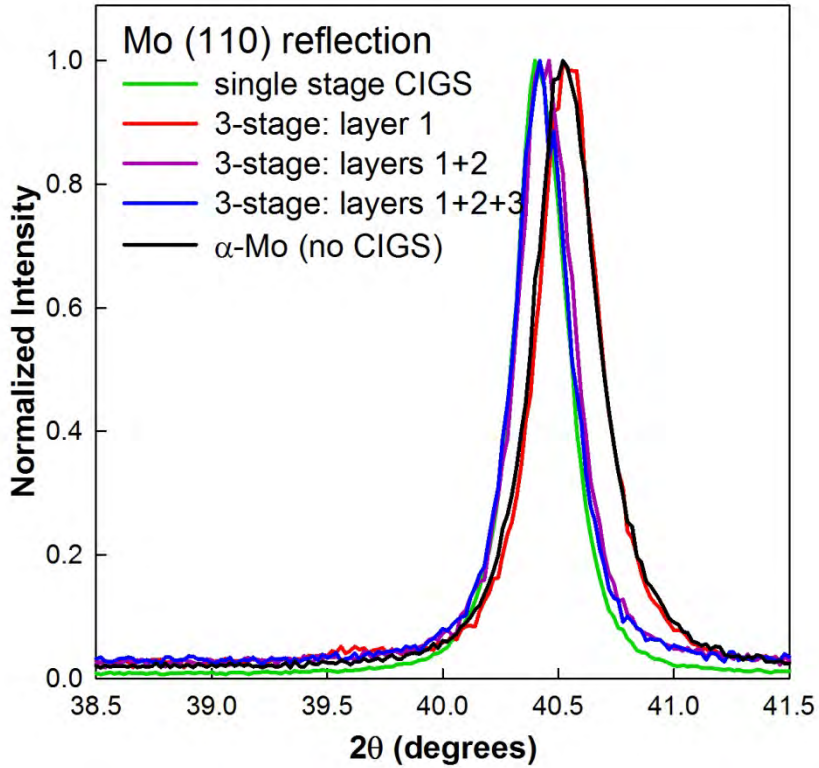

- The CIGS (220) peak from the single-stage sample appeared relatively symmetric, but the full three-stage sample as well as the sample interrupted following the second stage of growth showed significant peak anisotropy or doubling

Instrument standard

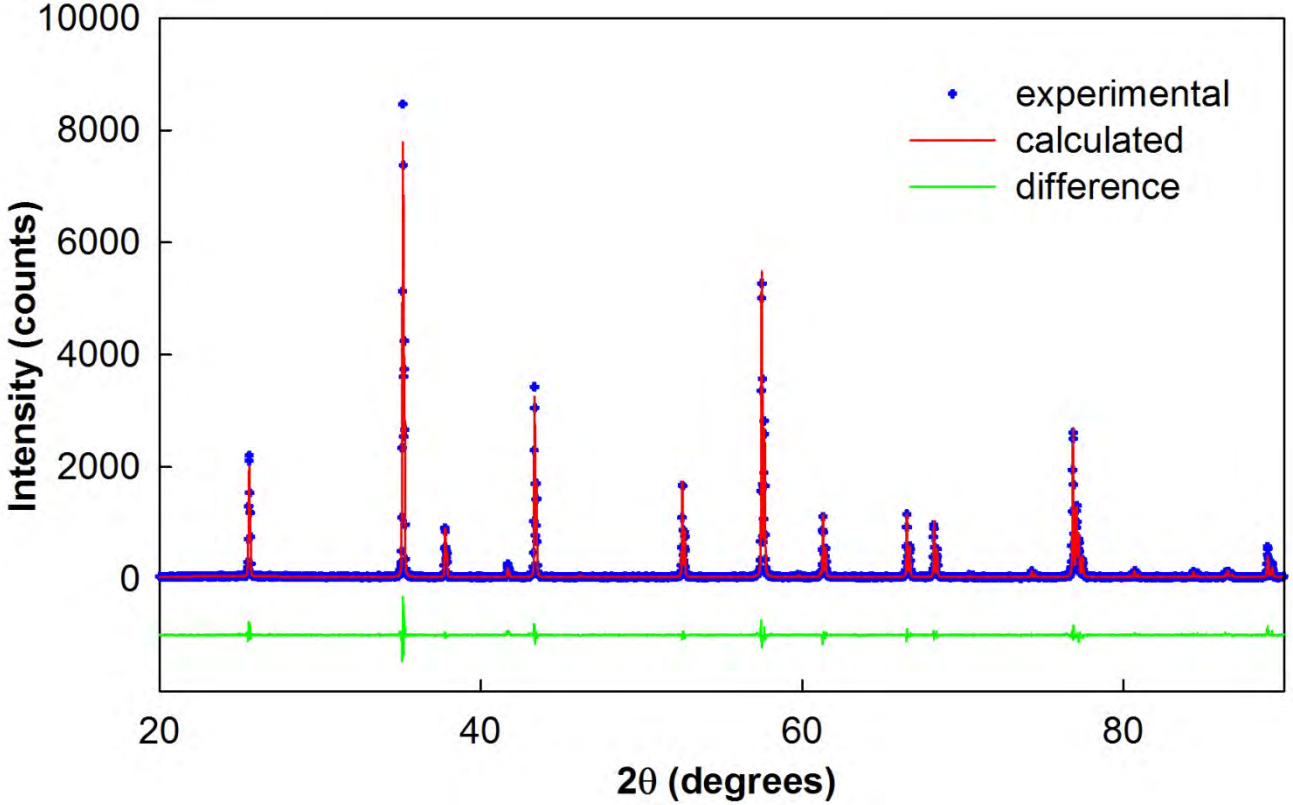

- SRM1976 (Al_2O_3) was used to determine the angle-dependent peak function and refinement of instrumental corrections such as axial divergence: $\sigma^2(2\theta) = U \tan 2\theta + V \tan \theta + W + P/\cos 2\theta$

Rietveld refinement of single-stage CIGS

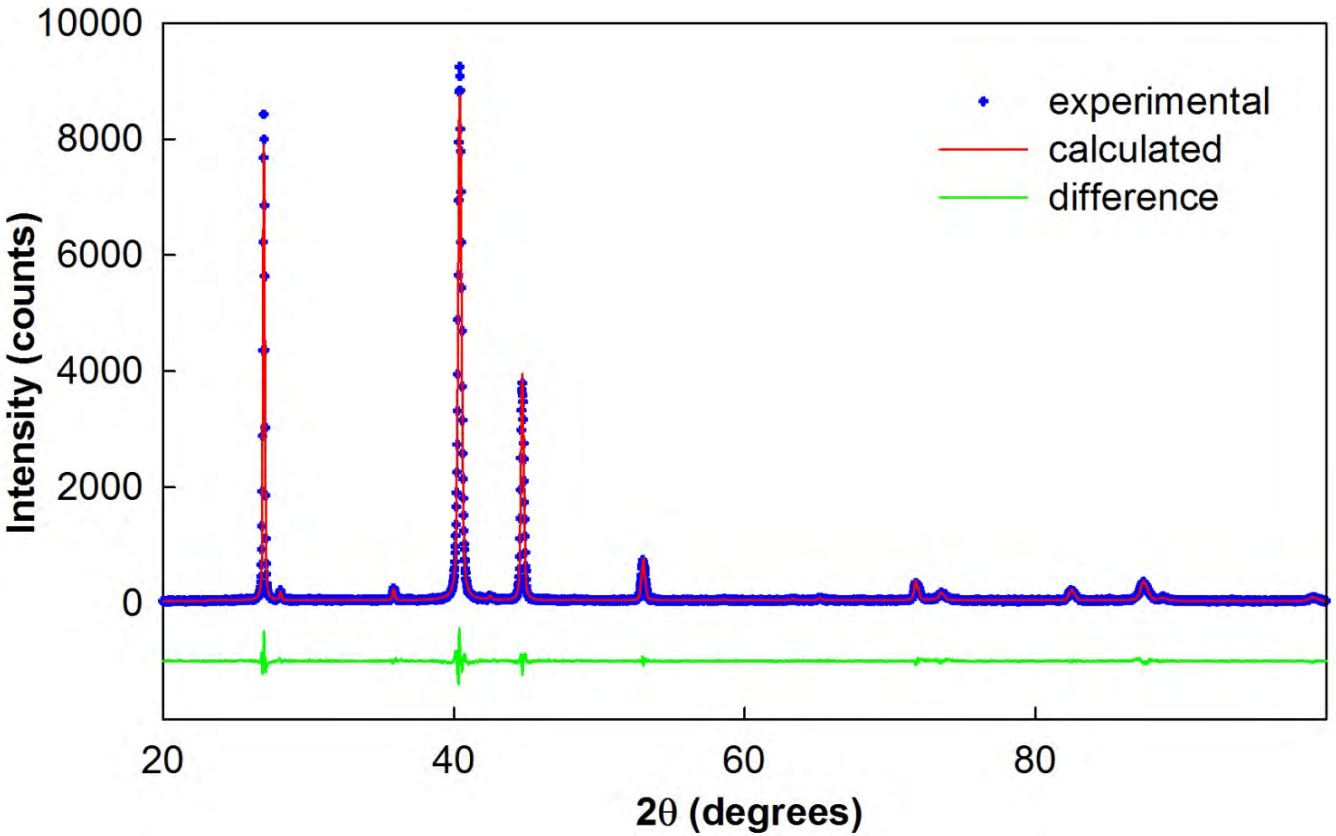

- The fit of the refined data to the experimental data is reasonably good, with a weighted residual (w_{RP}) of 11.3% and a goodness-of-fit (χ^2) of 1.63
- The refined gallium occupancy on In-Ga sublattice of 24% was in good agreement with X-ray fluorescence measurement of ~26% Ga.

Structure Evolution in Three-stage CIGS growth

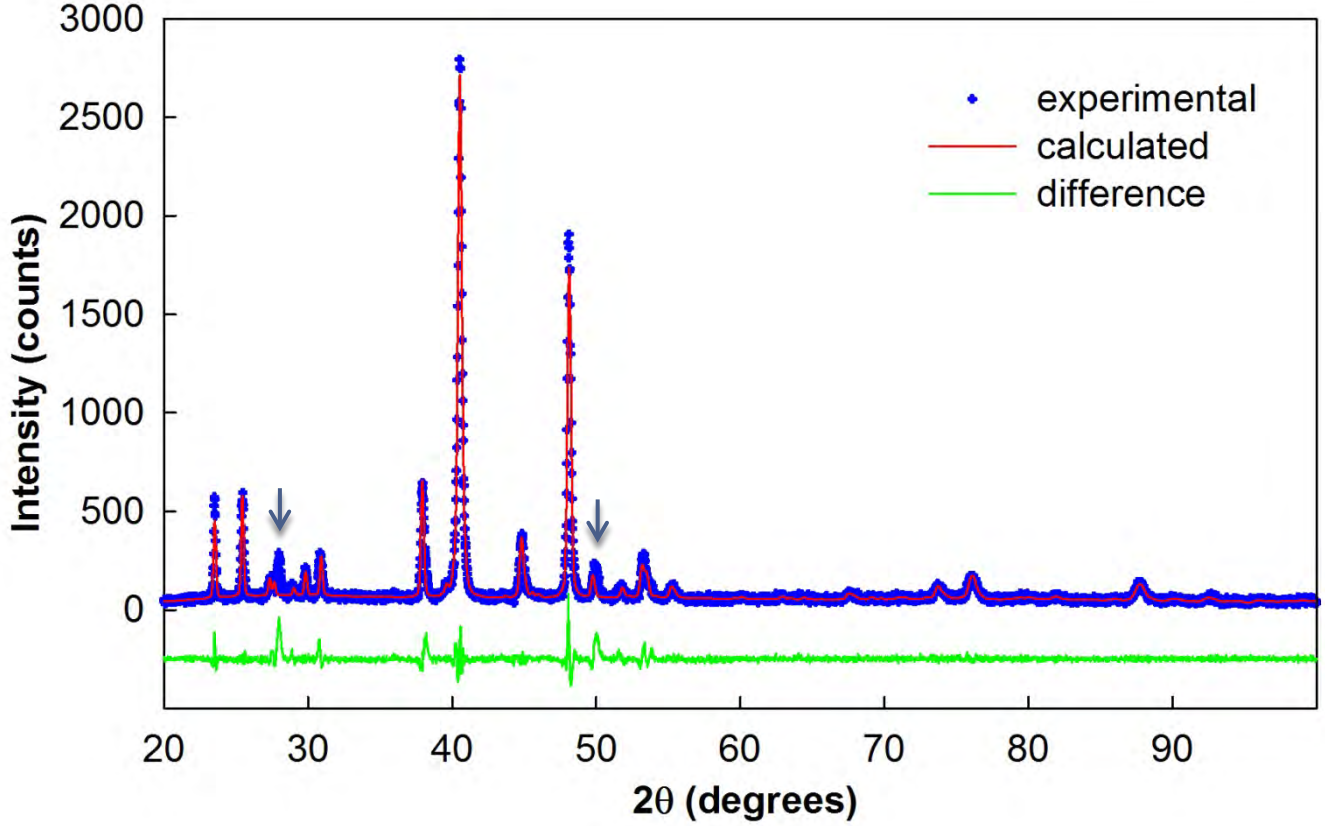

- Growth interruption at the first stage of the three-stage CIGS process shows primarily a $(Ga,In)_2Se_3$ phase ($P6_1$ space group)
- Other phase present → Pawley refinement

Structure Evolution in Three-stage CIGS growth

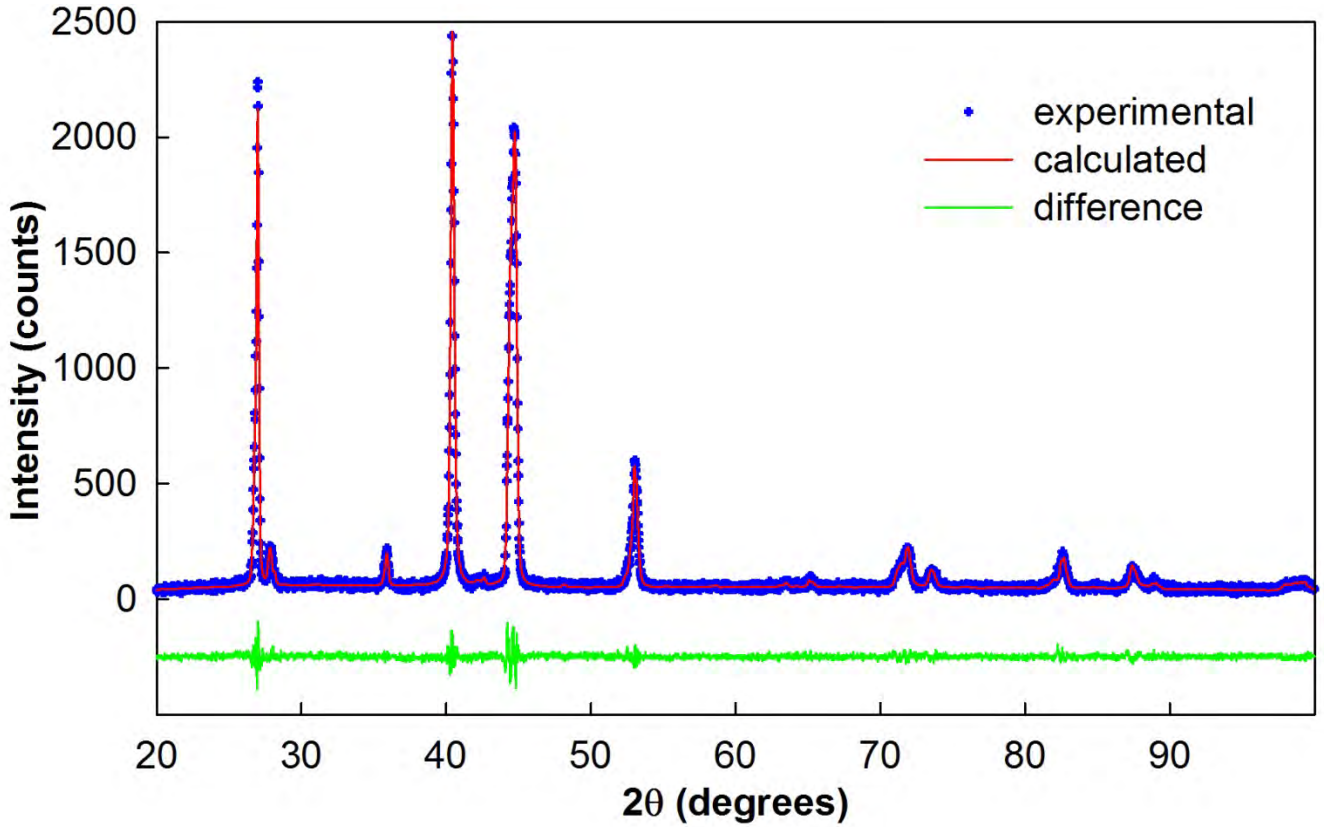

- Growth interruption at the second stage of the three-stage CIGS process is well fit with two tetragonal CIGS phase ($I\bar{4}2d$ space group) with different lattice parameters
- Full Rietveld refinement allows site occupancy determination

Summary of CIGS XRD Results

Sample	Phase and S.G.	Lattice constants (Å)	Fractional occupancy Cu	In	Ga	Se	L (nm)
Mo/SLG	α-Mo ($Im3m$)	a_o = 3.145	–				65
CIGS (single stage)	CIGS ($I\bar{4}2d$)	a_o = 5.734; c_o = 11.431	1	0.76	0.24	1	450
	α-Mo ($Im3m$)	a_o = 3.154	–				124
CIGS (three stage, 1st)	$(Ga,In)_2Se_3$ ($P6_1$)	a_o = 7.000; c_o = 19.354	Not available (Pawley)				?
	α-Mo ($Im3m$)	a_o = 3.147	–				103
CIGS (three stage, 1st+2nd)	CIGS1 ($I\bar{4}2d$)	a_o = 5.749, c_o = 11.609	1	0.81	0.19	1	300
	CIGS2 ($I\bar{4}2d$)	a_o = 5.730; c_o = 11.417	1	0.54	0.46	1	(300)
	α-Mo ($Im3m$)	a_o = 3.153	–				86
CIGS (three stage, 1st+2nd+3rd)	CIGS1 ($I\bar{4}2d$)	a_o = 5.733; c_o = 11.404	1	0.78	0.22	1	520
	CIGS2 ($I\bar{4}2d$)	a_o = 5.747; c_o = 11.521	1	0.51	0.49	1	(520)
	α-Mo ($Im3m$)	a_o = 3.155	–				90

- XRD shows an evolution of a large number of structural parameters
- "Three stage" deposition process involves a number of phases: this is not surprising!

A synchrotron-based *in situ* CIGS deposition

- A CIGS growth capability integrated into a synchrotron beamline would be the ideal tool for probing the kinetic factors that determine film structure and properties
- Ideal capability would permit both conventional and in-plane diffraction as well as X-ray reflectivity
- Capability for handling 10cm×10cm SLG or SS substrates would permit follow-on processing of PV devices

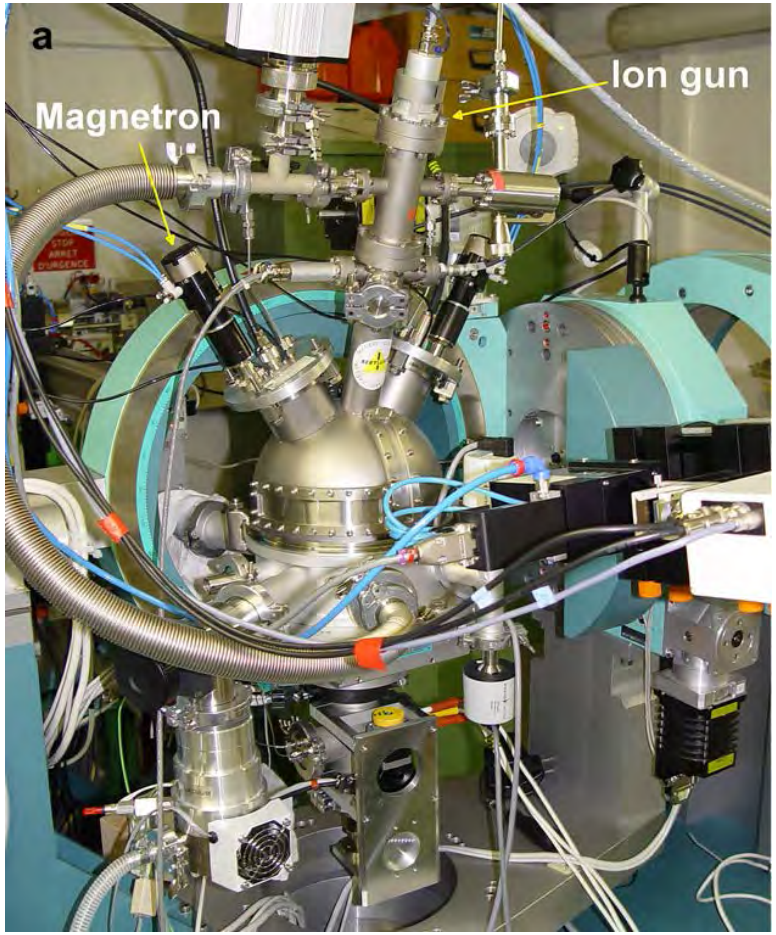

W. Matz *et al.*, "A two magnetron sputter deposition chamber for *in situ* observation of thin film growth by synchrotron radiation scattering" *Rev. Sci. Instr.*, **72**, 3344 (2001)

SUNY College of Nanoscale Science and Engineering

Combined EDXRD/XRF analysis of CIS growth

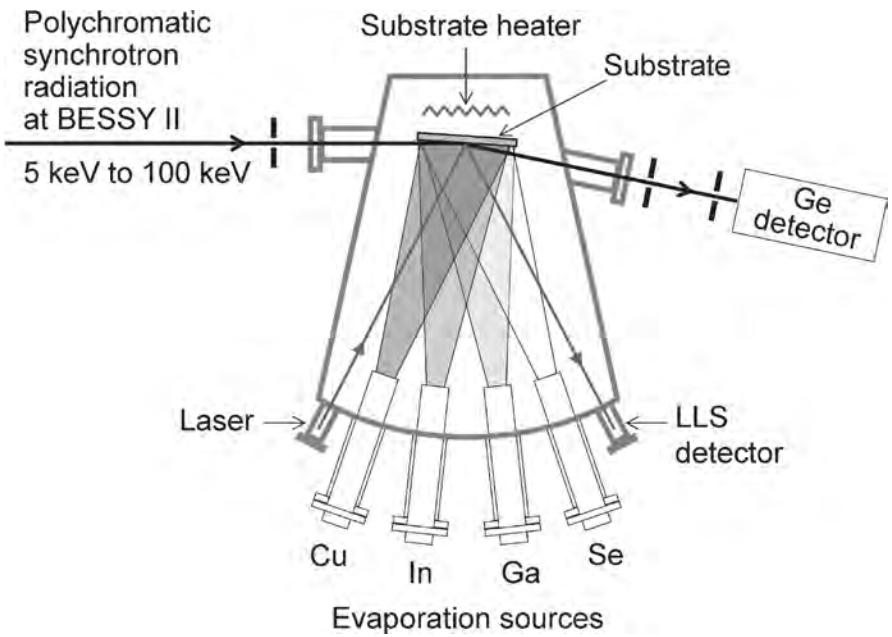

Rodriguez-Alvarez *et al.*, "Formation of $CuInSe_2$ and $CuGaSe_2$ Thin Films Deposited by Three-Stage Thermal Co-Evaporation: A Real-Time X-Ray Diffraction and Fluorescence Study" *Adv. Energy Mater.*, **2013**, *3*, 1381–1387

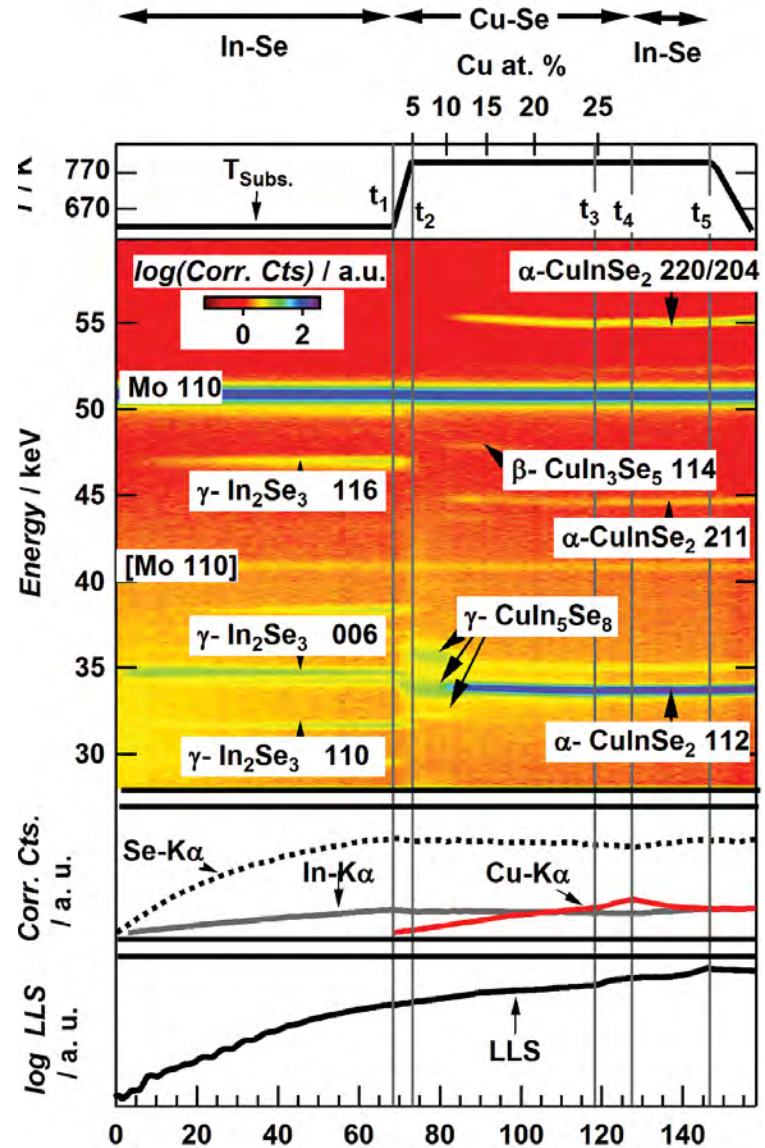

CIGS in situ characterization on the NSLS-II

- The high brilliance of the ISR beamline will permit structural and chemical characterization of CIGS materials with unprecedented precision
- Resonant Rietveld analyses can refine information on crystal chemistry in quaternary CIGS materials
- Real time characterization *in situ* during growth will allow the development of nanostructure and microstructure to be followed (reaction pathways and kinetics)
- Relate growth information to PV performance via collaboration with PVMC